Protein Arginine Deiminase 4: Evidence for a Reverse Protonation Mechanism†

Bryan Knuckley, Monica Bhatia, and Paul R. Thompson*

Department of Chemistry and Biochemistry, University of South Carolina, 631 Sumter Street, Columbia, South Carolina 29208

Received January 17, 2007; Revised Manuscript Received March 17, 2007

ABSTRACT: The presumed role of an overactive protein arginine deiminase 4 (PAD4) in the pathophysiology of rheumatoid arthritis (RA) suggests that PAD4 inhibitors could be used to treat an underlying cause of RA, potentially offering a mechanism to stop further disease progression. Thus, the development of such inhibitors is of paramount importance. Toward the goal of developing such inhibitors, we initiated efforts to characterize the catalytic mechanism of PAD4 and thereby identify important mechanistic features that can be exploited for inhibitor development. Herein we report the results of mutagenesis studies as well as our efforts to characterize the initial steps of the PAD4 reaction, in particular, the protonation status of Cys645 and His471 prior to substrate binding. The results indicate that Cys645, the active site nucleophile, exists as the thiolate in the active form of the free enzyme. pH studies on PAD4 further suggest that this enzyme utilizes a reverse protonation mechanism.

Rheumatoid Arthritis[1] (RA) is a chronic and progressive autoimmune disorder of unknown etiology. It is the second most common type of arthritis, affecting ∼1% of the adult US population and causing a mean reduction in life expectancy of 5−10 years (*1*, *2*). Because of its idiopathic nature, the therapeutic options available for RA largely focus on disease management, that is, treating its symptoms rather than treating the underlying cause(s) of the disease (*3*). Over the last several years, however, serological, genetic, and biochemical studies (*4*−*8*) have suggested a role for dysregulated protein arginine deiminase 4 (PAD4) activity in the onset and progression of this autoimmune disorder: PAD4 catalyzes the post-translational conversion of peptidyl-Arg to peptidyl-citrulline (Cit) (Figure 1). For example, RA associated mutations have been identified in the PAD4 gene (*4*), and autoantibodies that recognize citrullinated proteins are specifically produced by RA patients (*7*, *8*). Furthermore, the treatment of rodents with citrullinated collagen leads to a higher incidence and a faster rate of onset of collagen-induced arthritis in rodent models of RA (*9*, *10*). On the basis of this information, we and others have suggested that the deiminating activity of PAD4 is upregulated in RA patients, generating an aberrant immune response to citrullinated epitopes in the RA synovium (*5*, *11*, *12*). Thus, PAD4 inhibitors hold the promise of being effective therapeutics for RA. In addition to its presumed role in RA, dysregulated PAD4 activity and/or expression has recently been associated with the etiology of multiple sclerosis and cancer (*13*−*15*), thereby suggesting that the therapeutic value of PAD4 inhibitors could be broader than initially considered.

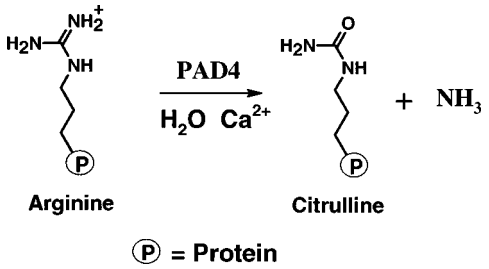

FIGURE 1: Reaction catalyzed by PAD4.

PAD4 is predominantly expressed in blood lymphocytes and has been suggested to play roles in apoptosis and differentiation (*4*, *16*−*19*). Additionally, PAD4 is known to be a calcium dependent nuclear enzyme that deiminates histones H2A, H3, and H4 and acts as a transcriptional corepressor for the estrogen receptor (*16*, *17*, *20*−*22*). However, and despite its importance as a therapeutic drug target, the physiological roles of PAD4 are incompletely defined and are only beginning to be deciphered. The recent development of potent and bioavailable PAD4 inhibitors and activity based protein profiling reagents (*23*−*25*) will undoubtedly be useful tools for obtaining a more complete description of the physiological role(s) of this enzyme.

Recent *in vitro* studies have generated significant data regarding the molecular details of PAD4 catalysis (although key gaps remain). For example, preliminary investigations have confirmed the identity and stoichiometry of the reaction products (*11*, *26*) and demonstrated that solvent oxygen is incorporated into the product, that is, peptidyl-Cit (*11*, *26*). Also, initial pH rate profiles performed with low substrate concentrations, approximating k_{cat}/K_m conditions, suggested that two ionizable groups were critical for catalysis (*11*). Finally, several structures of PAD4, determined by X-ray crystallography, have confirmed that PAD4 is a member of

† This work was supported in part by the start up funds from the University of South Carolina Research Foundation (to P.R.T.) and in part by National Institutes of Health Grant GM079357 (to P.R.T.).

* To whom correspondence should be addressed. Tel: (803)-777-6414. Fax: (803)-777-9521. E-mail: Thompson@mail.chem.sc.edu.

[1] Abbreviations: PAD, protein arginine deiminase; Cit, citrulline; RA, rheumatoid arthritis; BAEE, benzoyl L-arginine ethyl ester; BAA, benzoyl L-arginine amide; DTT, dithiothreitol; GST, glutathione *S*-transferase; TCEP, Tris(2-carboxyethyl)phosphine hydrochloride; HEPES, *N*-(2-hydroxyethyl)piperazine-*N*′-(2-ethanesulfonic acid); ADI, arginine deiminase; DDAH, dimethylarginine dimethylamino hydrolase; SIE, solvent isotope effect; SVE, solvent viscosity effect.

10.1021/bi700095s CCC: $37.00
Published on Web 05/12/2007

the amidinotransferase superfamily of enzymes (*27*−*29*). On the basis of this homology (*30*−*32*) and preliminary site directed mutagenesis experiments (*27*), there are four key catalytic residues, including Asp350, His471, and Asp473, that contribute to rate enhancement by playing loosely defined roles in substrate binding (Asp350 and Asp473) and general acid/general base catalysis (His471). Cys645, the fourth key catalytic residue, most likely acts as a nucleophile to generate a covalent *S*-alkylthiouronium intermediate akin to the acyl enzyme intermediates observed in other cysteine hydrolases. Note that while a kinetically competent covalent intermediate has yet to be demonstrated for PAD4, the fact that F- and Cl-amidine, two haloacetamidine-bearing mechanism based inactivators, irreversibly inactivate PAD4 by modifying Cys645 (*24*, *25*) argues forcefully for a role for Cys645 as the active site nucleophile when combined with the abundance of evidence for covalent catalysis among other amidinotransferase family members (e.g., rapid quench kinetic studies on arginine deiminase (ADI) (*33*), mass spectrometry studies on dimethylarginine dimethylaminohydrolase (DDAH) (*34*), and crystal structures of the *S*-alkylthiouronium intermediate in ADI (*31*)).

While at least four different mechanisms have been proposed to explain the deiminating activity of the various amidinotransferase family members (*11*, *30*−*32*, *35*), we initially proposed a working model that involves a nucleophilic thiolate whose charge is stabilized via an ion pair with His471, analogous to the Cys-imidazolium ion pair observed in papain (*36*). Herein we report the results of site directed mutagenesis studies, pK_a measurements on the active site thiol, pH rate profiles, and solvent isotope effects that support the existence of a nucleophilic active site thiolate. Furthermore, the results indicate that at the pH optimum only a small fraction of the enzyme exists in the catalytically competent thiolate form and in total suggest that PAD4 utilizes a reverse protonation mechanism (*37*, *38*).

EXPERIMENTAL PROCEDURES

Chemicals. Iodoacetamide and 2-chloroacetamidine were obtained from Oakwood Products (Columbia, SC). Dithiothreitol (DTT), iodoacetic acid, protease inhibitor cocktail (Cat#P8465), and Benzoyl L-arginine ethyl ester (BAEE) were acquired from Sigma-Aldrich (St. Louis, MO). Tris-(2-carboxyethyl)phosphine hydrochloride (TCEP) was obtained from Fluka. Dideuterium oxide was acquired from Cambridge Isotope Laboratories (Andover, MA).

Purification of PAD4. Recombinant human PAD4 was expressed and purified using methods analogous to previously described methods (*11*, *39*). Our optimized protocol is described in detail in the Supporting Information.

pH Profile. The pH profile of PAD4 was constructed by measuring the steady state kinetic parameters for the deimination of BAEE over a pH range of 6.0−9.0. Reaction buffers consisted of 100 mM Bis-Tris (5.7−7.5), 100 mM Tris-HCl (7.5−8.5), or 100 mM CHES (8.5−9.0) plus 2 mM DTT, 10 mM $CaCl_2$, 50 mM NaCl, and BAEE in various concentrations (0−20 mM in a final volume of 60 μL). Stock concentrations of BAEE were dissolved in 50 mM buffer at the desired pH. Enzyme assays were performed essentially as described in Kearney et al. (*11*). The initial rates obtained from these experiments were fit to eq 1

$$v = V_{max}[S]/(K_m + [S]) \quad (1)$$

using GraFit version 5.0.11 (*40*). The k_{cat} and k_{cat}/K_m values obtained from this analysis were plotted as a function of pH and fit to eq 2

$$y = ((Lim1 + Lim2 \times 10^{(pH-pK_{a1})})/(10^{(pH-pK_{a1})} + 1) - (((Lim2 - Lim3)) \times 10^{(pH-pK_{a2})})/(10^{(pH-pK_{a2})} + 1))) \quad (2)$$

using GraFit version 5.0.11. Lim1 is the amount of activity observed at low pH, lim2 is pH_{opt}, lim3 is the amount of activity observed at high pH.

Substrate Protection Experiments. Reaction mixtures containing 10 mM $CaCl_2$, 100 mM Tris-HCl at pH 7.6, 500 μM TCEP, 50 mM NaCl, and BAEE (2 mM or 10 mM) were preincubated with either 2-chloroacetamidine (5 mM) or iodoacetamide (1.25 mM) at 37 °C for 10 min. Subsequently, PAD4 (0.2 μM final) was added and aliquots (60 μL) were removed at various time points (0−15 min) and residual activity assayed as described above. Samples incubated without chloroacetamidine or iodoacetamide were used as controls. The data obtained were fit to eq 3

$$P = \frac{v_i}{k_{obs}}(1 - e^{(-k_{obs}*t)}) \quad (3)$$

using GraFit version 5.0.11. P is the amount of citrulline produced, v_i is the initial velocity, k_{obs} is the observed rate of inactivation, and t is the time.

Iodoacetamide Inactivation Kinetics. Inactivation reactions containing 500 μM TCEP, 10 mM $CaCl_2$, and 100 mM of buffer (pH 6.5 Bis-Tris, pH 7.6−9.0 Tris) were preincubated with 2.0 μM PAD4 for 10 min at 37 °C (20 μL total volume). Varying concentrations of iodoacetamide (0−2.0 mM) were then added. Inactivation reaction were quenched with DTT (20 mM final) at various time points (0−30 min) and then immediately added to a reaction mixture to measure the residual activity of PAD4. These reaction mixtures, which contained 10 mM $CaCl_2$, 50 mM NaCl, 100 mM Tris at pH 7.6, 2 mM DTT, and 10 mM BAEE (60 μL total volume), were preincubated at 37 °C for 10 min, before adding aliquots from the quenched inactivation mixture. Activity assays proceeded for 15 min at which point the reaction was stopped by flash freezing in liquid nitrogen. Residual enzymatic activity was then quantified using the methodology described above. The data obtained at each iodoacetamide concentration were fit to eq 4

$$v = v_o e^{-kt} \quad (4)$$

using Grafit version 5.0.11. v is the velocity, v_o is the initial velocity, k is the pseudo-first-order rate constant for inactivation, and t is time. Because of a lack of inactivator saturation, the second-order rate constant for enzyme inactivation, k_{inact}/K_I, was determined by plotting the observed inactivation rates (k_{obs}) versus inactivator concentration and fitting the data to eq 5

$$k_{obs} = \frac{k_{inact}}{K_I}[I] \quad (5)$$

using Grafit version 5.0.11. k_{inact} is the maximal rate of inactivation, K_I is the concentration of inactivator that yields

Table 1: Sequences of Forward and Reverse Primers for Site Directed Mutagenesis[a]

mutant	forward primer	reverse primer
H471A	tggctgtccgtgggcgccgtggacgagttc	gaactcgtccacggcgcccacggacagcca
H471G	tggctgtccgtgggcggcgtggacgagttc	gctcaggaactcgccgcccacggacagcca
H471Q	ctgtccgtgggccaggtggacgagttcctg	caggaactcgtccacctggcccacggacag
D350A	gaccagtggatgcaggccgaaatggagatcggc	gccgatctccatttcggcctgcatccactggtc
D350E	gaccagtggatgcaggaagaaatggagatcggc	gccgatctccatttcttcctgcatccactggtc
D350N	gaccagtggatgcagaatgaaatggagatcggctac	gtagccgatctccatttcattctgcatccactggtc
D473A	gtgggccacgtggccgagttcctgagc	gctcaggaactcggccacgtggcccac
D473E	gtccgtgggccacgtggaagagttcctgagctttg	caaagctcaggaactcttccacgtggcccacggac
D473N	gtccgtgggccacgtgaatgagttcctgagctttg	caaagctcaggaactcattcacgtggcccacggac
C645S	ggggaggtgcactccggcaccaacgtgc	gcacgttggtgccggagtgcacctcccc
C645A	ggggaggtgcacgccggcaccaacgtgc	gcacgttggtgccggcgtgcacctcccc

[a] All primers are written 5′ to 3′.

half-maximal inactivation, and [I] is the concentration of inactivator. The slopes thus obtained, that is, k_{inact}/K_I, were plotted versus pH and subsequently fit to eq 6

$$y = \frac{(Lim1 + Lim2)10^{(pH-pK_a)}}{10^{(pH-pK_a)} + 1} \quad (6)$$

using GraFit version 5.0.11. Lim1 is the minimum rate, and Lim2 is the maximum rate.

Iodoacetamide versus Iodoacetic Acid Inactivation Kinetics. Inactivation reactions containing 500 μM TCEP, 10 mM $CaCl_2$, and 100 mM HEPES at pH 7.6 were preincubated with 2.0 μM PAD4 at 37 °C (60 μL total volume). After 10 min, iodoacetamide or iodoacetic acid (1.25 mM) was added to the mixture. The residual activity of PAD4 was measured as described above.

2-Chloroacetamidine Inactivation Kinetics. Inactivation mixtures containing 2 mM DTT, 10 mM $CaCl_2$, and 100 mM of buffer (pH 6.5 MES, pH 7.0 to 9.0 Tris-HCl)) were preincubated with 2 μM PAD4 at 37 °C. After 10 min, 2-chloroacetamidine (0−30 mM) was added to the mixture. Residual activity was measured by removing aliquots from the inactivation mix at various time points (0 to 30 min). These aliquots were diluted 10-fold into reaction buffer (10 mM $CaCl_2$, 50 mM NaCl, 2 mM DTT, 100 mM Tris-HCl at pH 7.6, and 10 mM BAEE). The data were processed using the methods described above.

Site Directed Mutagenesis. Catalytic mutants of PAD4 were generated using the Quik Change Site Directed Mutagenesis Kit (Stratagene). The forward and reverse primers (IDT DNA technologies) used for each mutagenesis experiment are listed in Table 1. Note that the entire open reading frame of each mutant was sequenced to ensure that the proper mutation had been incorporated and that no additional mutations had been introduced during the PCR reaction. Mutant PAD4 enzymes were purified using the methodology described above.

Kinetic Studies on Mutant Enzymes. Steady state kinetic parameters for PAD4 mutants were determined as previously described. Because the catalytic activity of all of the mutants described in this study was significantly impaired relative to wild type PAD4, enzyme assays were performed with higher amounts of enzyme (2.5 μM final) and for longer time periods (2 h) to achieve detectable amounts of citrulline.

Solvent Isotope Effects. Solvent isotope effects (SIE) were measured in reaction buffers containing 50 mM Bis-Tris (pL 5.75−7.00), 50 mM Tris-HCl (pL 7.0−8.5), or 50 mM CHES (pL 8.5−9.0) as well as 10 mM $CaCl_2$, 2 mM DTT, 50 mM NaCl, PAD4, and various concentrations of BAEE (0−10 mM) in >96% D_2O. The kinetic parameters were determined using the methods described above. To control for possible solvent viscosity effects (SVE), the steady state kinetic parameters for the deimination of BAEE were determined under identical conditions at the pH optimum in assay buffer containing 10% glycerol. The SVE and SIE on the calcium dependence of PAD4 were also assessed as a further control. For these studies, PAD4 activity was measured in assay buffers containing either >96% D_2O or 10% glycerol plus $CaCl_2$ (0−10 mM), 50 mM Tris-HCl pH 7.6, 10 mM BAEE, 50 mM NaCl, 2 mM DTT, and PAD4. The $K_{0.5}$ for calcium was determined using the methodology described in Kearney et al. (*11*).

RESULTS

Site Directed Mutagenesis. To gain insight into the catalytic mechanism of PAD4, we generated a series of site specific mutations in the PAD4 gene at sites corresponding to Asp350, His471, Asp473, and Cys645, that is, the four key catalytic residues involved in substrate binding (Asp350 and Asp473), nucleophilic catalysis (Cys645), and general acid/general base catalysis (His471). Initially, all four residues were individually mutated to Ala, the proteins purified, and estimates of the kinetic parameters determined (Table S1, Supporting Information). In all cases, k_{cat}/K_m was decreased by greater than 7,900-fold, thereby indicating that all four residues are essential for catalysis, consistent with previous mutagenesis studies (*27*). Note that high concentrations of purified enzyme and extended incubation times were used to estimate k_{cat}/K_m and that partial proteolysis studies (Figure S1, Supporting Information), which are a sensitive indicator of PAD4 structure (*11*), were used to ensure that the lack of activity is not caused by a major structural perturbation, analogous to other systems (*41*−*43*).

To gain further insight into the roles of these residues in substrate binding and catalysis, a series of conservative mutations were generated. For example, a Cys → Ser mutant was generated for Cys645; Asp → Asn and Glu mutants were generated for Asp350 and Asp473; and a His → Gln mutant was generated for His471. The enzymatic activity of the Cys645Ser and His471Gln mutants was decreased by greater than 14,000- and 34,000-fold (Table S1, Supporting Information), respectively, consistent with the essential roles of these residues in nucleophilic and general acid/base catalysis.

Somewhat surprisingly, mutation of Asp350 and Asp473 to Asn and Glu led to very dramatic declines in PAD4 activity, on the order of those observed for the Asp → Ala mutations (Table S1, Supporting Information). These results indicate that PAD4 activity is sensitive to even conservative mutations and further suggest that the correct positioning of the guanidinium group, with respect to the active site Cys, and charge neutralization are critical determinants of catalytic power. Overall, the lack of activity observed with these mutants may be due to a lack of synergy between these four key catalytic residues.

Note that the lack of activity was not due to a gross conformational change because all of the mutants behaved in a manner similar to that of wild type enzyme in our partial proteolysis assay (Figure S1, Supporting Information). Also note that the studies described herein are consistent with the fact that active site mutations in a related enzyme, arginine deiminase (ADI) from *Pseudomonas aeruginosa*, lead to similar decreases in deiminating activity (*44*). Finally, the specific effects of the mutations described above on each of the two half reactions, that is, intermediate formation and intermediate hydrolysis, are unknown but will be the subject of future investigations.

pH Studies. To further probe the PAD4 reaction mechanism, pH rate profiles were determined for wild type enzyme. These studies were pursued because pH rate profiles can suggest the identity of catalytically important functional groups in the free enzyme (k_{cat}/K_m vs pH), the ES complex (k_{cat} vs pH), or the substrate (k_{cat}/K_m vs pH) (*45*, *46*). For these studies, pH profiles were constructed by measuring the steady state kinetic parameters for the deimination of BAEE over a range of pH values (5.7−9.0). Note that BAEE is a synthetic substrate that is commonly used to study PAD activity. Also note that there is essentially no effect on the calcium dependence of PAD4 over this pH range and that PAD4 activity is linear with respect to time at all pH values used in this study (*11*).

The plots of log k_{cat}/K_m versus pH are bell-shaped and fit well to a model with two apparent pK_a values and a limiting nonzero plateau (133 M^{-1} s^{-1}) for the ascending limb (Figure 3A). The apparent pK_a values of the ascending and descending limbs are 6.9 ± 0.2 (slope of 0.68) and 9.0 ± 0.1 (slope of −1.15), respectively. Note that because these pK_a values are within 3 units, they must be considered apparent pK_a values. Therefore, the corrected values, calculated according to the method of Segel (*47*), are 7.3 and 8.2 for the ascending and descending limbs, respectively. Although not definitive, the presence of a nonzero plateau for the ascending limb could suggest that a second ionization form of the enzyme is active at low pH. The plots of k_{cat} versus pH are similarly bell-shaped and fit well to a model with two apparent pK_a values and limiting nonzero plateaus of 0.76 s^{-1} for the ascending limb and 0.24 s^{-1} for the descending limb (Figure 3B). The apparent pK_a values of the ascending and descending limbs are 7.0 ± 0.3 (slope of 0.37) and 8.7 ± 0.4 (slope of −0.60), respectively. The pK_a values obtained from this analysis most likely represent the protonation states of His471 and Cys645 in the ES complex (Figure 2); although considering the stepwise nature of the reaction mechanism, it is difficult to definitively assign either of these values to a particular residue.

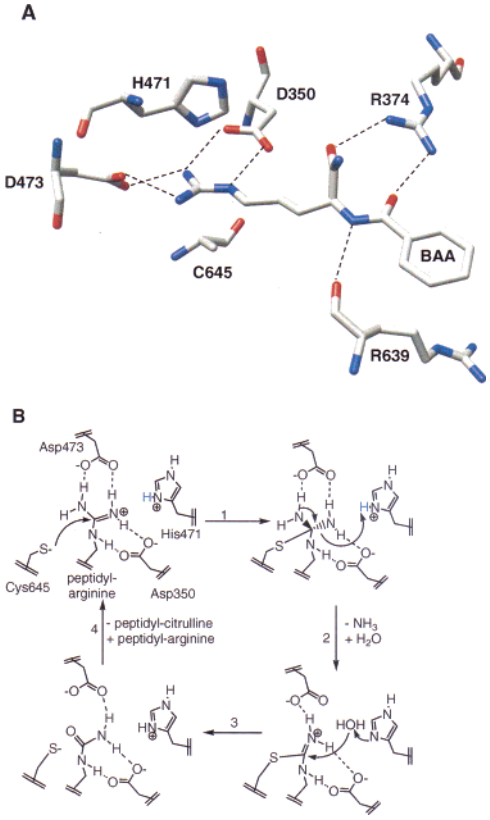

FIGURE 2: (A) Active site of PAD4. (B) Working model of PAD4 catalysis. A possible mechanism of PAD4 catalysis involves a nucleophilic thiolate (step 1), and His 471 acts as a general acid, donating a proton to the departing amine during the collapse of the first tetrahedral intermediate (step 2). This leads to the formation of an *S*-alkyl thiouronium intermediate. The exchange of a molecule of water for ammonia occurs, and, as drawn, His471 acts as a general base to activate a water molecule for nucleophilic attack on the thiouronium intermediate (step 3). This leads to the formation of the second tetrahedral intermediate that collapses to eliminate the Cys thiolate and in the process generate Cit. Asp473 is appropriately positioned to deprotonate the hydroxyl. Step 4 involves the exchange of product for substrate.

pK_a Measurements on the Active Site Cysteine (Cys645) by Iodoacetamide Inactivation Kinetics. On the basis of the structure and proposed mechanism of PAD4, the simplest assumption is that the ascending limb in the k_{cat}/K_m versus pH plots corresponds to the formation of the active site thiolate, that is, the deprotonation of Cys645, and that the descending limb corresponds to the deprotonation of His471, that is, the pK_a values of Cys645 and His471 are 7.3 and 8.2, respectively. However, an alternative possibility is the special case of a reverse protonation mechanism (*37*, *38*). In such a mechanism, the pK_a assignments are the reverse of the simplest assumption, that is, the pK_a values of Cys645 and His471 are 8.2 and 7.3, respectively.

To distinguish between these two possibilities, direct measurements of the Cys645 side chain pK_a were made by determining the rates of iodoacetamide induced enzyme inactivation over a range of pH values (pH 6.5 to pH 9) and concentrations of iodoacetamide, similar to related systems (*48*, *49*). The percentage of activity remaining after iodoacetamide treatment was determined as a function of time, and the resulting plots were fit to a single exponential to determine the pseudo-first-order rate constant for inactivation, that is, k_{obs}. Figure 4A depicts a representative plot of the

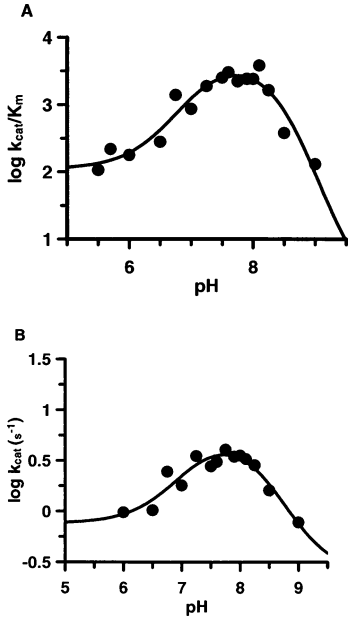

FIGURE 3: (A) Plot of log k_{cat}/K_m versus pH. (B) Plot of log k_{cat} versus pH.

data, obtained at pH 7.6. Plots of k_{obs} versus iodoacetamide concentration were linear, indicating second-order inactivation kinetics (Figure 4B). The second-order rate constants of inactivation, that is, k_{inact}/K_I, obtained at each of the indicated pH values were subsequently plotted against pH, and as depicted in Figure 4C, the results indicate that the rate of PAD4 inactivation increases with rising pH. Graphical analyses are consistent with a single pK_a value of 8.3 ± 0.07. This pK_a value is in excellent agreement with that obtained for the descending limb in the k_{cat}/K_m versus pH rate profiles, suggesting that PAD4 utilizes a reverse protonation mechanism.

Note that two sets of control experiments were performed to confirm that the iodoacetamide induced inactivation of PAD4 was due to the modification of an active site residue, that is, Cys645. First, the rates of iodoacetamide and iodoacetic acid induced PAD4 inactivation were compared. The results demonstrate that PAD4 is preferentially inactivated by iodoacetamide (Figure 5A). The fact that iodoacetic acid is a relatively poorer PAD4 inactivator is at least partially consistent with the modification of an active site residue because electrostatic repulsions between Asp350 and Asp473 and iodoacetic acid would be expected to inhibit the interaction between this compound and PAD4. Second, the rate of iodoacetamide induced inactivation is higher at lower concentrations of substrate (Figure 5B). This result is also consistent with the modification of an active site residue because substrate binding would be expected to preclude inactivator binding.

pK_a Measurements on the Active Site Cysteine (Cys645) by 2-Chloroacetamidine Inactivation Kinetics. The pK_a of Cys645 was also measured with 2-chloroacetamidine, a positively charged PAD4 inactivator, by determining the rates of enzyme inactivation over a range of pH values (pH 6.5 to pH 9) and concentrations. As described above for the iodoacetamide induced inactivation of PAD4, the percentage of activity remaining after 2-chloroacetamidine treatment was determined as a function of time, and the resulting plots were fit to a single exponential to determine the pseudo-first-order

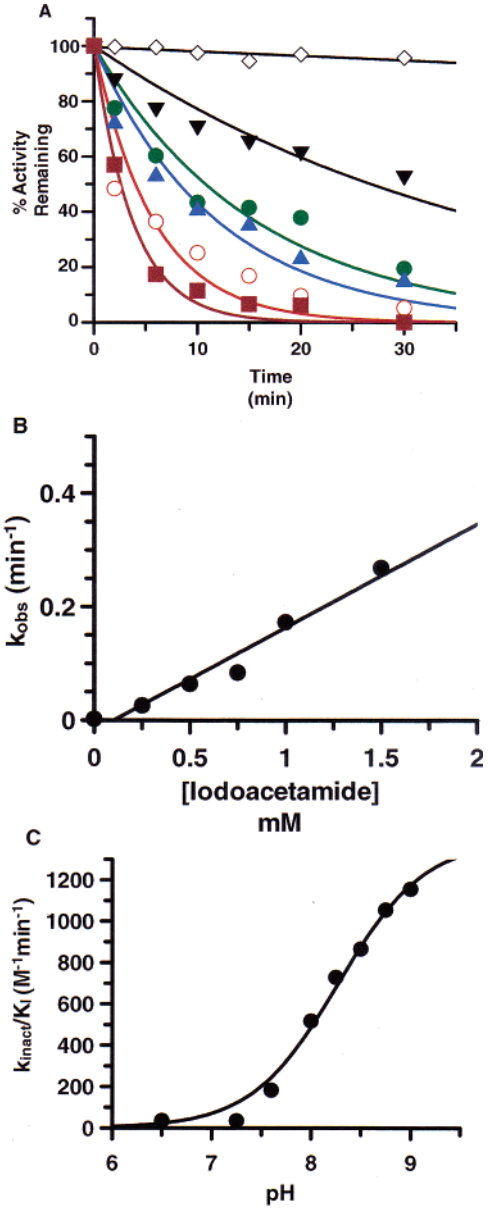

FIGURE 4: Time and concentration dependent inactivation of PAD4 by iodoacetamide. (A) observed inactivation at pH 7.6 by different concentrations of iodoacetamide: 0 (◇), 250 (▼), 500 (●), 750 (▲), 1000 (○), and 1500 μM (■). (B) The pseudo-first-order rate constant of PAD4 inactivation is plotted vs iodoacetamide concentration, and the plots were fitted to eq 5 as described in materials and methods. (C) pK_a of C645. Second-order rate constants were plotted vs pH and fit to eq 6 as described in Experimental Procedures.

rate constant for inactivation, that is, k_{obs}, at each concentration of inactivator (Figure 6A). Plots of k_{obs} versus 2-chloroacetamidine concentration were linear within the concentration range used (Figure 6B), and gratifyingly, the second-order rate constant for PAD4 inactivation, 55 ± 6.0 M^{-1} min^{-1} at pH 7.6, is quite close to that reported by the Fast group (35 M^{-1} min^{-1}) (*39*). Plots of k_{inact}/K_I versus pH (Figure 6C) reveal that the pK_a of Cys645 is 7.9 ± 0.16, in good agreement with both the descending limb of the k_{cat}/K_m versus pH rate profiles and that obtained via iodoacetamide inactivation kinetics. Furthermore, these results indicate that this positively charged inactivator has only minimal effects on the pK_a of the Cys645 thiol. Note that the substrate could protect against PAD4 inactivation by 2-chloroaceta-

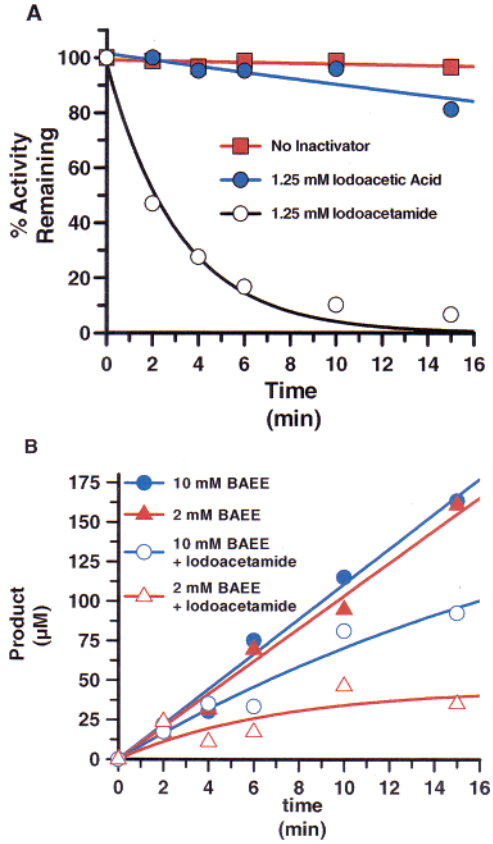

FIGURE 5: Inactivation of PAD4 with iodoacetamide. (A) Iodoacetamide is a better PAD4 inactivator than iodoacetic acid. Percent activity remaining was plotted vs time and fit to eq 4 as described in Experimental Procedures. (B) Substrate protects against iodoacetamide-induced inactivation of PAD4. Plots of product formation vs time are depicted for PAD4 in the absence and presence of iodoacetamide (1.25 mM) at two different concentrations of BAEE (2 and 10 mM).

midine (Figure 6D), consistent with the modification of an active site residue.

Solvent Isotope Effects (SIEs). Because PAD4 catalyzes a hydrolysis reaction that involves a nucleophilic thiolate, we evaluated the SIE by performing the reaction in D_2O over a range of pL values. The SIE on k_{cat} was normal with a k_{cat}^{H}/k_{cat}^{D} of 1.25 at the pL optimum, indicating that proton abstraction does not contribute significantly to the rate-limiting step of the reaction. In contrast to the normal SIE on k_{cat}, an inverse SIE was observed for k_{cat}/K_m over the entire pL range studied (Figure 7). At the pL optimum, the ratio $k_{cat}/K_m^{H}/k_{cat}/K_m^{D}$ was 0.43. Inverse SIEs of this type have previously been used to support the existence of a thiolate−imidazolium ion pair (*50*−*54*).

Note that under identical conditions, the concentration of calcium required for half-maximal activity, that is, the $K_{0.5}$, was virtually unaffected (0.56 ± 0.04 for H_2O (*11*) vs 1.0 ± 0.4 for D_2O), thereby indicating that the inverse SIE is unlikely to be due to a change in the calcium dependence of the enzyme. Also, note that a normal SVE on both k_{cat} (1.32) and k_{cat}/K_m (1.34) was observed when the steady state kinetic parameters were determined in the presence of 10% glycerol (w/v), a concentration of glycerol that closely matches the viscosity of D_2O (*55*), thereby indicating that the inverse SIE is not due to an increase in the viscosity of buffers containing D_2O.

Scheme 1 : Binding of Inactivator to Either the E-SH (Upper Pathway) or E-S^- (Lower Pathway) Complexes

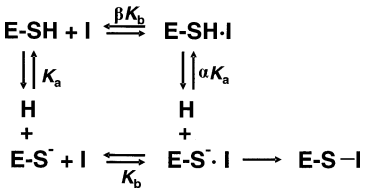

DISCUSSION

On the basis of the structure of PAD4 and literature precedents from related systems (*30*−*32*), we initially proposed a working model of PAD4 catalysis that involved a nucleophilic thiolate (Figure 2; (*11*)) and hypothesized that this species was stabilized via the formation of an ion pair with His471, analogous to the thiolate−imidazolium ion pair observed in papain (*36*). To begin to test the validity of this hypothesis, we generated a series of semi-conservative and nonconservative active site mutants (Cys → Ala and Ser; His → Gly, Ala, Gln) designed to directly evaluate the roles of Cys645 and His471. Although the activity associated with these mutant enzymes is negligible (k_{cat}/K_m ↓ by ≥7,900-fold), the results are nevertheless consistent with an essential role for these residues in PAD4 catalysis and are consistent with the proposed mechanism, that is, that a nucleophilic thiolate and properly oriented imidazole group[2] are required for nucleophilic and general acid/base chemistry, respectively. Similar results have been obtained for other amidinotransferase family members, for example, ADI (*44*).

pH rate profiles (k_{cat}/K_m versus pH) were also constructed to identify and characterize the roles of catalytically important residues, and the results are consistent with the presence of two key ionizable groups with pK_a values of 7.3 and 8.2. On the basis of the proposed catalytic mechanism, these pK_a values most likely correspond to the protonation states of His471 and Cys645 before the substrate has bound to the enzyme. To more definitively assign one of these pK_a values to Cys645, pK_a measurements were made on the active site thiol by determining the effect of pH on the rate of PAD4 inactivation by iodoacetamide and 2-chloroacetamidine. As described above, the rates of inactivation increased with pH for both compounds, and in both cases, the pK_a determined for Cys645 is quite close to the value obtained for the descending limb of the k_{cat}/K_m versus pH rate profile, that is, pH 8.2. The fact that the pK_a of Cys645 corresponds to the descending limb of the k_{cat}/K_m versus pH rate profile is most consistent with a reverse protonation mechanism (see above) and thereby suggests that the pK_a of His471 is ∼7.3.

The fact that the iodoacetamide and 2-chloroacetamidine inactivation kinetics yield similar pK_a valuess for Cys645 is inconsistent with a *pure* substrate assisted mechanism of thiol deprotonation.[3] This is the case because in a pure substrate assisted mechanism, binding to the thiol form of the enzyme (i.e., E-SH, where E is the enzyme, and SH is the thiol; upper pathway in Scheme 1) is obligatory. Therefore, if 2-chloroacetamidine, a guanidinium analogue, forms this initial encounter complex (i.e., E-SH−2-chloroacetamidine), a

[2] The activity of neither the His471Gly nor the His471Ala mutant could be chemically rescued by the addition of a variety of imidazole- and guanidinium-containing compounds.

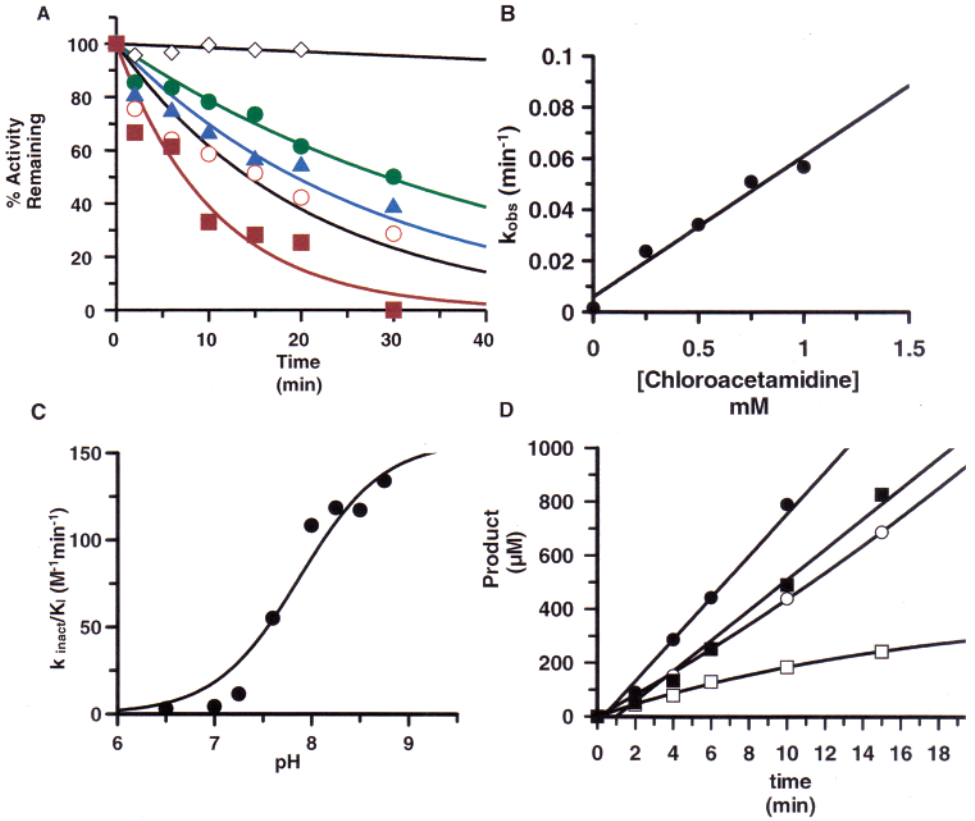

FIGURE 6: Time and concentration dependent inactivation of PAD4 by 2-chloroacetamidine. (A) Observed inactivation at pH 7.6 by different concentrations of 2-chloroacetamidine: 0 (◇), 250 (●), 500 (▲), 1000 (○), and 1500 μM (■). (B) Pseudo-first-order rate constant of PAD4 inactivation is plotted vs 2-chloroacetamidine concentration, and plots were fitted to eq 5 as described in Experimental Procedures. (C) pK_a of C645. Second-order rate constants were plotted vs pH and fit to eq 6 as described in Experimental Procedures. (D) Substrate protects against 2-chloroacetamidine induced inactivation of PAD4. Plots of product formation vs time are depicted for PAD4 in the absence or presence of 2-chloroacetamidine (5 mM) at two different concentrations of PAD4: 10 mM BAEE (●), 2 mM BAEE (■), 10 mM BAEE with 2-chloroacetamidine (○), and 2 mM BAEE with 2-chloroacetamidine (□).

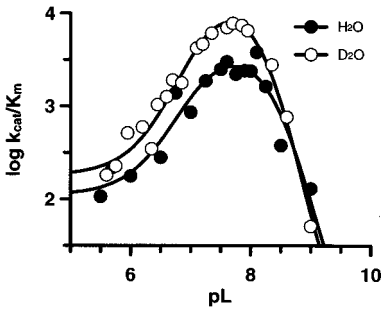

FIGURE 7: Solvent isotope effect (SIE). Plots of log k_{cat}/K_m vs pL in H_2O (●) or D_2O (○).

reasonable assumption given that 2-chloroacetamidine displays saturation kinetics at the pH optimum (*39*), the observed pK_a should have shifted dramatically from the resting state by the factor α. Although an effect on the k_{inact}/K_I titration curve may not be apparent if 2-chloroacetamidine does not form an initial encounter complex with E-SH or if the inactivator can bind to either the thiol or thiolate forms of the enzyme (i.e., binding to E-SH is not obligatory), the results obtained are most consistent with preferential binding of this positively charged inactivator to the thiolate form of the enzyme at the pH optimum via the lower pathway in Scheme 1, that is, a reverse protonation mechanism.

A reverse protonation mechanism is also supported by the fact that the decrease in k_{cat}/K_m at both pH extremes is largely driven by an increase in K_m. Although effects of pH on K_m are often difficult to interpret, large changes in K_m as a function of pH are consistent with the preferential binding of substrate to one form of the enzyme at the pH optimum (*47*). Thus when taken in combination, our results are most consistent with substrate binding to a form of the enzyme that consists of a negatively charged thiolate and a positively charged imidazolium ion, that is, the ES^-H^+ form, where E is the enzyme, S^- is the thiolate, and H^+ is the imidazolium ion. This appears to be the case, despite the fact that only a small fraction of PAD4 (~15% of the enzyme) exists as ES^-H^+ at the pH optimum because the titration curves for His471 and Cys645 are overlapping (Figure 8).

If substrate binds preferentially to the ES^-H^+ form of PAD4 at the pH optimum, as our data suggests, it is likely that the negative charge of the thiolate is at least partially stabilized via the formation of an ion pair with the imidazolium ion. Such an interaction would be important because the PAD4 active site is highly anionic (Asp350 and Asp473 should be deprotonated), disfavoring thiolate formation, and His471 is the only positively charged residue within the

[3] In a substrate assisted mechanism of thiol deprotonation, the proximity of the positively charged substrate guanidinium to a high pK_a active site Cys promotes thiol deprotonation by either an unknown general base or by proton donation to solvent (*59*). The term *pure* is used to indicate that the substrate can only bind to the enzyme when Cys645 exists as the thiol (Scheme 1, upper pathway) and is also used to differentiate between the possibility that the substrate can bind to the enzyme regardless of whether Cys645 exists as the thiol or thiolate, that is, substrate can bind via either pathway in Scheme 1.

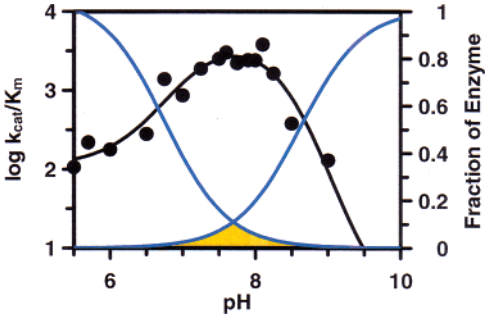

FIGURE 8: Fraction of enzyme in the active form (yellow) with C645 deprotonated and H471 protonated, i.e., E-S$^-$H$^+$.

vicinity of Cys645 that could serve this function. The inverse SIE on k_{cat}/K_m is consistent with the dissociation of a proton from a thiol with a fractionation factor of less than 1, and such inverse SIEs have previously been used to support the existence of a thiolate−imidazolium ion pair in other Cys hydrolases (*50*−*54*). The inverse SIE on k_{cat}/K_m is also noteworthy because it is inconsistent with previously proposed mechanisms (*27*, *35*, *56*) that involve His471 acting as a general base to deprotonate the substrate guanidinium, which subsequently deprotonates the thiol, because if such a mechanism were operative, a normal SIE would be expected.

Although the distance between the imidazole nitrogen of His471 and the β-carbon of Cys645 is 6.9 Å in the structure of the PAD4C645A−calcium complex (the best available representation of active PAD4 before substrate has bound; pdb ID 1WD9), it is important to recognize that the true distance between these two residues is likely to be considerably shorter. For example, on the basis of the length of a C−S bond (~1.6 Å), the distance between this nitrogen and the thiolate is likely less than ~5.3 Å. Furthermore, at the pH used for protein crystallization (pH 8.0) and considering the reverse protonation mechanism described above, this structure represents less than 10% of active PAD4; thus, the distance may appear large because this structure actually represents an average of inactive conformers.

Implications for Other Amidinotransferase Family Members. PAD4 belongs to a large superfamily of guanidinium-modifying enzymes, and despite shared active site architectures, differences in specific active site residues and kinetic properties exist between members of the amidinotransferase superfamily of enzymes. For example, (i) the pH optimum of various family members varies significantly from <pH 5.5 for *Pseudomonas aeruginosa* ADI to pH 7.6 for PAD4 (*11*, *30*, *57*, *58*); (ii) the active site Cys in DDAH appears to be deprotonated via a substrate assisted mechanism (*59*); (iii) the distance between the imidazolium ion and the active site Cys is considerably longer in both ADI and DDAH; (iv) PAD4 requires high concentrations of DTT to maintain activity, whereas other amidinotransferase family members do not (*11*, *39*, *44*); and (v) PAD4 has a His-Cys dyad, whereas ADI and DDAH possess a His-Cys-Glu catalytic triad. Thus, the ion pair mechanism proposed herein for PAD4 may not be universally utilized by other amidinotransferase family members.

In summary, our results indicate that in the free and active form of the enzyme, Cys645 exists as the thiolate. Furthermore, pH studies and pK_a measurements with iodoacetamide and 2-chloroacetamidine strongly suggest that PAD4 utilizes a reverse protonation mechanism. These studies have already aided our successful efforts to synthesize PAD4 inhibitors (*23*−*25*) and will undoubtedly serve as a guide to others interested in developing a PAD4 targeted RA pharmaceutical.

SUPPORTING INFORMATION AVAILABLE

Supplementary methods, supplementary Table 1, and supplementary Figure 1. This material is available free of charge via the Internet at http://pubs.acs.org.

REFERENCES

1. Akil, M., and Amos, R. S. (1995) ABC of rheumatology: rheumatoid arthritis I: clinical features and diagnosis, *Br. Med. J. 310*, 587−590.
2. Finesilver, A. G. (2003) Newer approaches to the treatment of rheumatoid arthritis. *Wis. Med. J. 102*, 34−37.
3. Smolen, J. S., and Steiner, G. (2003) Therapeutic strategies for rheumatoid arthritis, *Nat. Rev. Drug. Discovery 2*, 473−488.
4. Suzuki, A., Yamada, R., Chang, X., Tokuhiro, S., Sawada, T., Suzuki, M., Nagasaki, M., Nakayama-Hamada, M., Kawaida, R., Ono, M., Ohtsuki, M., Furukawa, H., Yoshino, S., Yukioka, M., Tohma, S., Matsubara, T., Wakitani, S., Teshima, R., Nishioka, Y., Sekine, A., Iida, A., Takahashi, A., Tsunoda, T., Nakamura, Y., and Yamamoto, K. (2003) Functional haplotypes of PADI4, encoding citrullinating enzyme peptidylarginine deiminase 4, are associated with rheumatoid arthritis, *Nat. Genet. 34*, 395−402.
5. Vossenaar, E. R., Zendman, A. J., van Venrooij, W. J., and Pruijn, G. J. (2003) PAD, a growing family of citrullinating enzymes: genes, features and involvement in disease, *BioEssays 25*, 1106−1118.
6. Vossenaar, E. R., and Van Venrooij, W. J. (2004) Citrullinated proteins: sparks that may ignite the fire in rheumatoid arthritis, *Arthritis Res. Ther. 6*, 107−111.
7. Schellekens, G. A., de Jong, B. A., van den Hoogen, F. H., van de Putte, L. B., and van Venrooij, W. J. (1998) Citrulline is an essential constituent of antigenic determinants recognized by rheumatoid arthritis-specific autoantibodies, *J. Clin. Invest. 101*, 273−281.
8. Schellekens, G. A., Visser, H., de Jong, B. A., van den Hoogen, F. H., Hazes, J. M., Breedveld, F. C., and van Venrooij, W. J. (2000) The diagnostic properties of rheumatoid arthritis antibodies recognizing a cyclic citrullinated peptide, *Arthritis Rheum. 43*, 155−163.
9. Lundberg, K., Nijenhuis, S., Vossenaar, E. R., Palmblad, K., van Venrooij, W. J., Klareskog, L., Zendman, A. J., and Harris, H. E. (2005) Citrullinated proteins have increased immunogenicity and arthritogenicity and their presence in arthritic joints correlates with disease severity, *Arthritis Res. Ther. 7*, R458−R467.
10. Kuhn, K. A., Kulik, L., Tomooka, B., Braschler, K. J., Arend, W. P., Robinson, W. H., and Holers, V. M. (2006) Antibodies against citrullinated proteins enhance tissue injury in experimental autoimmune arthritis, *J. Clin. Invest. 116*, 961−973.
11. Kearney, P. L., Bhatia, M., Jones, N. G., Luo, Y., Glascock, M. C., Catchings, K. L., Yamada, M., and Thompson, P. R. (2005) Kinetic characterization of protein arginine deiminase 4: a transcriptional corepressor implicated in the onset and progression of rheumatoid arthritis, *Biochemistry 44*, 10570−10582.
12. Thompson, P. R., and Fast, W. (2006) Histone citrullination by protein arginine deiminase: is arginine methylation a green light or a roadblock? *ACS Chem. Biol. 1*, 433−441.
13. Moscarello, M. A., Mastronardi, F. G., and Wood, D. D. (2007) The role of citrullinated proteins suggests a novel mechanism in the pathogenesis of multiple sclerosis, *Neurochem. Res. 32*, 251−256.
14. Mastronardi, F. G., Wood, D. D., Mei, J., Raijmakers, R., Tseveleki, V., Dosch, H. M., Probert, L., Casaccia-Bonnefil, P., and Moscarello, M. A. (2006) Increased citrullination of histone H3 in multiple sclerosis brain and animal models of demyelination: a role for tumor necrosis factor-induced peptidylarginine deiminase 4 translocation, *J. Neurosci. 26*, 11387−11396.
15. Chang, X., and Han, J. (2006) Expression of peptidylarginine deiminase type 4 (PAD4) in various tumors, *Mol. Carcinog. 45*, 183−196.

16. Cuthbert, G. L., Daujat, S., Snowden, A. W., Erdjument-Bromage, H., Hagiwara, T., Yamada, M., Schneider, R., Gregory, P. D., Tempst, P., Bannister, A. J., and Kouzarides, T. (2004) Histone deimination antagonizes arginine methylation, *Cell 118*, 545−553.
17. Wang, Y., Wysocka, J., Sayegh, J., Lee, Y. H., Perlin, J. R., Leonelli, L., Sonbuchner, L. S., McDonald, C. H., Cook, R. G., Dou, Y., Roeder, R. G., Clarke, S., Stallcup, M. R., Allis, C. D., and Coonrod, S. A. (2004) Human PAD4 regulates histone arginine methylation levels via demethylimination, *Science 306*, 279−283.
18. Liu, G. Y., Liao, Y. F., Chang, W. H., Liu, C. C., Hsieh, M. C., Hsu, P. C., Tsay, G. J., and Hung, H. C. (2006) Overexpression of peptidylarginine deiminase IV features in apoptosis of haematopoietic cells, *Apoptosis 11*, 183−196.
19. Lee, Y. H., Coonrod, S. A., Kraus, W. L., Jelinek, M. A., and Stallcup, M. R. (2005) Regulation of coactivator complex assembly and function by protein arginine methylation and demethylimination, *Proc. Natl. Acad. Sci. U.S.A. 102*, 3611−3616.
20. Nakashima, K., Hagiwara, T., and Yamada, M. (2002) Nuclear localization of peptidylarginine deiminase V and histone deimination in granulocytes, *J. Biol. Chem. 277*, 49562−49568.
21. Hagiwara, T., Nakashima, K., Hirano, H., Senshu, T., and Yamada, M. (2002) Deimination of arginine residues in nucleophosmin/B23 and histones in HL-60 granulocytes, *Biochem. Biophys. Res. Comm. 290*, 979−983.
22. Hagiwara, T., Hidaka, Y., and Yamada, M. (2005) Deimination of histone H2A and H4 at arginine 3 in HL-60 granulocytes, *Biochemistry 44*, 5827−5834.
23. Luo, Y., Knuckley, B., Bhatia, M., and Thompson, P. R. (2006) Activity based protein profiling reagents for protein arginine deiminase 4 (PAD4): synthesis and in vitro evaluation of a fluorescently-labeled probe, *J. Am. Chem. Soc. 128*, 14468−14469.
24. Luo, Y., Knuckley, B., Lee, Y. H., Stallcup, M. R., and Thompson, P. R. (2006) A fluoro-acetamidine based inactivator of protein arginine deiminase 4 (PAD4): design, synthesis, and in vitro and in vivo evaluation, *J. Am. Chem. Soc. 128*, 1092−1093.
25. Luo, Y., Arita, K., Bhatia, M., Knuckley, B., Lee, Y. H., Stallcup, M. R., and Thompson, P. R. (2006) Inhibitors and inactivators of protein arginine deiminase 4: functional and structural characterization, *Biochemistry 45*, 11727−11736.
26. Hidaka, Y., Hagiwara, T., and Yamada, M. (2005) Methylation of the guanidino group of arginine residues prevents citrullination by peptidylarginine deiminase IV, *FEBS Lett. 579*, 4088−4092.
27. Arita, K., Hashimoto, H., Shimizu, T., Nakashima, K., Yamada, M., and Sato, M. (2004) Structural basis for Ca^{2+}-induced activation of human PAD4, *Nat. Struct. Mol. Biol. 11*, 777−783.
28. Arita, K., Shimizu, T., Hashimoto, H., Hidaka, Y., Yamada, M., and Sato, M. (2006) Structural basis for histone N-terminal recognition by human peptidylarginine deiminase 4, *Proc. Natl. Acad. Sci. U.S.A. 103*, 5291−5296.
29. Shirai, H., Mokrab, Y., and Mizuguchi, K. (2006) The guanidino-group modifying enzymes: structural basis for their diversity and commonality, *Proteins 64*, 1010−1023.
30. Galkin, A., Lu, X., Dunaway-Mariano, D., and Herzberg, O. (2005) Crystal structures representing the Michaelis complex and the thiouronium reaction intermediate of *Pseudomonas aeruginosa* arginine deiminase, *J. Biol. Chem. 280*, 34080−34087.
31. Das, K., Butler, G. H., Kwiatkowski, V., Clark, A. D., Jr., Yadav, P., and Arnold, E. (2004) Crystal structures of arginine deiminase with covalent reaction intermediates; implications for catalytic mechanism, *Structure 12*, 657−667.
32. Murray-Rust, J., Leiper, J., McAlister, M., Phelan, J., Tilley, S., Santa Maria, J., Vallance, P., and McDonald, N. (2001) Structural insights into the hydrolysis of cellular nitric oxide synthase inhibitors by dimethylarginine dimethylaminohydrolase, *Nat. Struct. Biol. 8*, 679−683.
33. Lu, X., Galkin, A., Herzberg, O., and Dunaway-Mariano, D. (2004) Arginine deiminase uses an active-site cysteine in nucleophilic catalysis of L-arginine hydrolysis, *J. Am. Chem. Soc. 126*, 5374−5375.
34. Stone, E. M., Person, M. D., Costello, N. J., and Fast, W. (2005) Characterization of a transient covalent adduct formed during dimethylarginine dimethylaminohydrolase catalysis, *Biochemistry 44*, 7069−7078.
35. Shirai, H., Blundell, T. L., and Mizuguchi, K. (2001) A novel superfamily of enzymes that catalyze the modification of guanidino groups, *Trends Biochem. Sci. 26*, 465−468.
36. Lewis, S. D., Johnson, F. A., and Shafer, J. A. (1981) Effect of cysteine-25 on the ionization of histidine-159 in papain as determined by proton nuclear magnetic resonance spectroscopy. Evidence for a his-159−Cys-25 ion pair and its possible role in catalysis, *Biochemistry 20*, 48−51.
37. Frankel, B. A., Kruger, R. G., Robinson, D. E., Kelleher, N. L., and McCafferty, D. G. (2005) *Staphylococcus aureus* sortase transpeptidase SrtA: insight into the kinetic mechanism and evidence for a reverse protonation catalytic mechanism, *Biochemistry 44*, 11188−11200.
38. Mock, W. L., and Stanford, D. J. (2002) Anisylazoformylarginine: a superior assay substrate for carboxypeptidase B type enzymes, *Bioorg. Med. Chem. Lett. 12*, 1193−1194.
39. Stone, E. M., Schaller, T. H., Bianchi, H., Person, M. D., and Fast, W. (2005) Inactivation of two diverse enzymes in the amidinotransferase superfamily by 2-chloroacetamidine: dimethylargininase and peptidylarginine deiminase, *Biochemistry 44*, 13744−13752.
40. Leatherbarrow, R. J. (2004) *GraFit*, Version 5.0.11, Erathicus Software, Staines, UK.
41. Thompson, P. R., Schwartzenhauer, J., Hughes, D. W., Berghuis, A. M., and Wright, G. D. (1999) The COOH terminus of aminoglycoside phosphotransferase (3′)-IIIa is critical for antibiotic recognition and resistance, *J. Biol. Chem. 274*, 30697−30706.
42. Thompson, P. R., Boehr, D. D., Berghuis, A. M., and Wright, G. D. (2002) Mechanism of aminoglycoside antibiotic kinase APH-(3′)-IIIa: role of the nucleotide positioning loop, *Biochemistry 41*, 7001−7007.
43. Boehr, D. D., Thompson, P. R., and Wright, G. D. (2001) Molecular mechanism of aminoglycoside antibiotic kinase APH-(3′)-IIIa. Roles of conserved active site residues, *J. Biol. Chem. 276*, 23929−23936.
44. Lu, X., Li, L., Wu, R., Feng, X., Li, Z., Yang, H., Wang, C., Guo, H., Galkin, A., Herzberg, O., Mariano, P. S., Martin, B. M., and Dunaway-Mariano, D. (2006) Kinetic analysis of *Pseudomonas aeruginosa* arginine deiminase mutants and alternate substrates provides insight into structural determinants of function, *Biochemistry 45*, 1162−11672.
45. Cleland, W. W. (1982) The use of pH studies to determine chemical mechanisms of enzyme-catalyzed reactions, *Methods Enzymol. 87*, 390−405.
46. Dixon, M., and Webb, E. C. (1964) *Enzymes*, Academic Press, New York.
47. Segel, I. H. (1975) *Enzyme Kinetics: Behavior and Analysis of Rapid Equilibrium and Steady-State Enzyme Systems*, Wiley-Interscience, New York.
48. Zhang, Z. Y., and Dixon, J. E. (1993) Active site labeling of the Yersinia protein tyrosine phosphatase: the determination of the pKa of the active site cysteine and the function of the conserved histidine 402, *Biochemistry 32*, 9340−9345.
49. Lohse, D. L., Denu, J. M., Santoro, N., and Dixon, J. E. (1997) Roles of aspartic acid-181 and serine-222 in intermediate formation and hydrolysis of the mammalian protein-tyrosine-phosphatase PTP1, *Biochemistry 36*, 4568−4575.
50. Quinn, D. M., and Sutton, L. D. (1991) Theoretical Basis and Mechanistic Utility of Solvent Isotope Effects, in *Enzyme Mechanism from Isotope Effects* (Cook, P. F., Ed.) pp 73−126, CRC Press, Boca Raton, FL.
51. Wandinger, A., and Creighton, D. J. (1980) Solvent isotope effects on the rates of alkylation of thiolamine models of papain, *FEBS Lett. 116*, 116−121.
52. Brocklehurst, K., Kowlessur, D., Patel, G., Templeton, W., Quigley, K., Thomas, E. W., Wharton, C. W., Willenbrock, F., and Szawelski, R. J. (1988) Consequences of molecular recognition in the S1-S2 intersubsite region of papain for catalytic-site chemistry. Change in pH-dependence characteristics and generation of an inverse solvent kinetic isotope effect by introduction of a P1-P2 amide bond into a two-protonic-state reactivity probe, *Biochem. J. 250*, 761−772.
53. Polgar, L. (1974) Mercaptide-imidazolium ion-pair: the reactive nucleophile in papain catalysis, *FEBS Lett. 47*, 15−18.
54. Polgar, L. (1979) Deuterium isotope effects on papain acylation. Evidence for lack of general base catalysis and for enzyme−leaving-group interaction, *Eur. J. Biochem. 98*, 369−374.
55. Karsten, W. E., Lai, C. J., and Cook, P. F. (1995) Inverse solvent isotope effects in the NAD-Malic enzyme reaction are the result of the viscosity difference between D_2O and H_2O: implications for solvent isotope effect studies, *J. Am. Chem. Soc. 117*, 5914−5918.

56. Galkin, A., Kulakova, L., Sarikaya, E., Lim, K., Howard, A., and Herzberg, O. (2004) Structural insight into arginine degradation by arginine deiminase, an antibacterial and parasite drug target, *J. Biol. Chem. 279*, 14001−14008.
57. Lu, X., Li, L., Wu, R., Feng, X., Li, Z., Yang, H., Wang, C., Guo, H., Galkin, A., Herzberg, O., Mariano, P. S., Martin, B. M., and Dunaway-Mariano, D. (2006) Kinetic analysis of *Pseudomonas aeruginosa* arginine deiminase mutants and alternate substrates provides insight into structural determinants of function, *Biochemistry 45*, 1162−1172.
58. Weickmann, J. L., Himmel, M. E., Smith, D. W., and Fahrney, D. E. (1978) Arginine deiminase: demonstration of two active sites and possible half-of-the-sites reactivity, *Biochem. Biophys. Res. Commun. 83*, 107−113.
59. Stone, E. M., Costello, A. L., Tierney, D. L., and Fast, W. (2006) Substrate-assisted cysteine deprotonation in the mechanism of dimethylargininase (DDAH) from *Pseudomonas aeruginosa*, *Biochemistry 45*, 5618−5630.

BI700095S